VLBI Observations of a Complete Sample of Radio Galaxies V. 3C346 and 4C31.04: two Unusual CSS Sources.

W. D. Cotton[1], L. Feretti[2,3], G. Giovannini[2,3], T. Venturi[2], L. Lara[4], J. Marcaide[5], and A. E. Wehrle[6]

[1]National Radio Astronomy Observatory, 520 Edgemont Road, Charlottesville, VA 22903-2475
[2]Istituto di Radioastronomia del CNR, Via P. Gobetti 101, I-40129 Bologna, Italy.
[3]Dipartimento di Astronomia, Universitá di Bologna, via Zamboni 33, I-40100 Bologna, Italy.
[4]Instituto de Astrofísica de Andalucía, CSIC, Apdo. 3004, 18080 Granada, Spain.
[5]Departamento de Astronomía, Universitat de València, 46100 Burjassot, Spain.
[6]Infrared Processing and Analysis Center, California Institute of Technology, M/S 100-22, Pasadena, CA 91125.

Accepted for the publication in the *Astrophysical Journal*, October 20th 1995 issue

ABSTRACT

We present observations at 1.7 and 8.4 GHz of two Compact Steep Spectrum (CSS) sources from a complete sample of low-intermediate power radio galaxies. 3C346 shows an asymmetric structure with a one-sided "jet" and "hot spot". Present observations suggest that the classification of this source as a CSS is inappropriate, and that it is a common radio galaxy at a small angle to the line of sight. Its properties are in agreement with the predictions of unified schemes models. 4C31.04 shows more complex structure with the possibility of a centrally located flat spectrum core in between two close lobes. We suggest that this source could be a low redshift Compact Symmetric Object.

Subject Headings: radio continuum: galaxies - Galaxies: jets - Galaxies: nuclei

1. INTRODUCTION

In recent years, the parsec scale radio structure of high power radio galaxies and quasars has been extensively studied using Very Long Baseline Interferometry (VLBI). In order to test unified scheme models and understand the nuclear properties of radio sources, a complete statistical study of well defined samples, as well as detailed analyses of individual sources are necessary. In addition, to effectively determine the morphological characteristics of the parsec scale structures, observations at multiple frequencies are needed to distinguish the nature of the different components of these sources. In this paper we present results on two sources, 3C346 and 4C31.04, taken from a larger sample of radio galaxies (Giovannini *et al.* 1990). Nearly simultaneous VLBI observations were obtained for them at 1.7 and 8.4 GHz.

VLBI mapping and analysis of all the radio galaxies in our sample is in progress (see Giovannini *et al.* 1994 and references therein). The two radio sources which we present in this paper are classified, on the basis of their kiloparsec scale structures, as Compact Steep Spectrum (CSS) sources (Peacock & Wall 1982, Fanti *et al.* 1990). The origin and evolution of this class of sources is not yet well understood. On the basis of statistical arguments, Fanti *et al.*, (1990) argue that sources of this class are predominantly intrinsically small rather than apparently small due to projection effects. It is not yet clear whether these sources are the early stages of more extended sources or whether the interstellar medium in the host galaxies is so dense that the radio sources cannot escape from the confines of the galaxy.

The detailed study of the two sources discussed here will add new information about the objects in this class. Additionally, it is a step towards the completion of the VLBI study of our sample of radio galaxies.

3C346 (B 1641+174) is identified with an elliptical galaxy with redshift 0.162. It shows, at arcsecond and sub-arcsecond resolution, a compact core component from which a one sided jet emerges toward the east, extending for ∼4.5". An extended structure is present, both around the jet and on the opposite side, for a total extent of ∼12". The prominence of the compact core and the amorphous nature of the extended structure suggest to Spencer *et al.* (1991) that this source is a larger source viewed nearly end on. Confirmation that this source does not belong in the CSS class will improve the statistical analysis of that class by removing a non member. This result can also test the current unified schemes models since, according to these models, a high power radio galaxy viewed at a small angle with respect to the line of sight would appear as a quasar like object.

4C31.04 (B 0116+319) is identified with a nearby (z=0.059) elliptical galaxy. The small distance to this CSS source allows a detailed study of its parsec scale structure and a comparison of its properties with more distant and powerful CSS sources. Wrobel & Simon (1986) give 0.327 GHz VLBI results finding the source resolved into a double separated by about 0.07". This result makes 4C31.04 a good candidate for the new class of sources named Compact Symmetric Objects (CSO, see Readhead *et al.* 1994 for a recent review). The astrophysical importance of these sources is discussed in recent papers (see e.g. Wilkinson *et al.* 1994, Readhead *et al.* 1995). Since the number of known CSOs is very low and up to now all are very powerful objects with a large redshift, identification of a nearby CSO might open new possibilities for a more detailed study of the physical properties of this class of sources. $H_0 = 100$ km sec^{-1}Mpc^{-1} and $q_0 = 1$ is assumed throughout the paper.

2. OBSERVATIONS AND DATA REDUCTION

The sources under study were observed in 1992 January – February using 7 Very Long

Baseline Array (VLBA) telescopes, one Very Large Array (VLA) telescope and, when possible, the antennas of Medicina, Noto and Madrid (Deep Space Network, DSS65) in Europe (see Table 1).

Data were obtained with the MkII VLBI recording system and correlated on the Caltech/JPL Block 2 correlator in Pasadena. Amplitude calibration was carried out on the basis of measured system temperatures and assumed antenna sensitivities and correlator efficiencies. The gain calibration was tested by observing the two VLBI calibrator sources 0133+476 and 1739+522 several times during the experiment. Both sources were observed nearly simultaneously at the VLA in order to derive their total flux density. 0133+476 was marginally resolved on all the baselines used. Its measured flux density at 1.7 and 8.4 GHz was 1.38 Jy and 0.97 Jy, respectively. A self calibrated model of 0133+476 accounting for the total flux density was used in the amplitude calibration. 1739+522 was used only to calibrate the 3C346 8.4 GHz data set, and it turned out to be slightly resolved only on the transatlantic baselines. Its total flux density measured with the VLA at this frequency was 2.45 Jy.

2.1 3C346

3C346 was observed at 1.7 GHz using only the US telescopes, since due to scheduling and technical problems the 3 European telescopes were not available. The 8.4 GHz observations were made using all telescopes but DSS65. At this frequency, the source was not detected on baselines to Medicina. The uv coverages obtained on 3C346 are given in Figure 1a,b. Since the antennas used at 8.4 GHz were mostly located in the southwestern United States with two antennas in Europe, there is a large hole in the middle of the coverage.

Editing of data, amplitude calibration and the initial passes of self calibration were performed in the Caltech VLBI package (Pearson 1991). Fringe fitting, final self calibration and analysis was performed in the NRAO Astronomical Image Processing System (AIPS). Fringe fitting used the global method of Schwab & Cotton (1983) with a solution interval of 10 minutes.

The data at both frequencies were first model fitted by means of the program MODELFIT in the Caltech Package. This stage proved to be essential, since it allowed us to locate the more diffuse easternmost component and to estimate its total flux density. The best models obtained with the model fitting at each frequency were used to start the self calibration. The initial self calibration iterations adjusted only antenna phases but the final iteration adjusted antenna gains as well. We used a short solution interval (2 - 10 seconds) in the phase self calibration cycles and a longer solution interval (2 hours) in the last self calibration iteration.

At 8.4 GHz only the "core" region could be seen in the full resolution image (HPBW = 2.5×1 milliarcsec PA = $0°$). We therefore made a lower resolution image (HPBW = 23.5 milliarcsec) by applying a taper in the uv plane in order to reveal the lower surface brightness lobe regions. Parameters relevant to the maps and source are given in Table 2. In this table the total flux density (S_T) is obtained from the sum of the CLEAN components, the core flux density (S_c) is the peak brightness of the core (assuming it to be much smaller than the beam) and the "jet" flux density is obtained from the integral over a region containing the visible portion of the jet up to 2 arcseconds from the core. Since the methods of measuring these components are different, the sum of the core and jet flux densities do not equal the total but agree within the uncertainties.

2.2 4C31.04

The 1.7 GHz observations of 4C31.04 were made with the US telescopes and Medicina.

The uv coverage is given in Figure 2a. The source was undetected on the baselines to Medicina. As the calibrator source 0133+476, located near the source and observed between the scans of 4C31.04, was detected on all baselines, the non-detection was assumed to be due to source resolution.

All post correlation analysis was performed in the NRAO AIPS package. Fringe fitting used the global method of Schwab & Cotton (1983) with a solution interval of 12 minutes. The self calibration iterative procedure for 4C31.04 was started using a point source model.

The 8.4 GHz observations of 4C31.04 were made using all telescopes but Medicina (see Table 1). The uv coverage obtained on 4C31.04 at 8.4 GHz is shown in Figure 2b. Fringe fitting used the model obtained at 1.7 GHz. Since 4C31.04 is strongly resolved, the fringe fitting solutions were smoothed with a median window filter and failed solutions were replaced by interpolated values of good solutions. There were no detections of the source on any baselines involving Noto or DSS65 and only occasional detections involving the VLBA antennas at North Liberty and Brewster. Again, the calibrator source was observed many times in between the source scans and always detected on all baselines so the non detections are assumed to be due to the resolution of 4C31.04.

Only phases were adjusted in the self calibration process, which was started with the model derived from the 1.7 GHz observations. Since the source was undetected on long baselines, we tapered the uv data using a Gaussian function that drops to 30% at 20 million wavelengths, and data from projected baselines longer than 30 million wavelengths were excluded; the resulting synthesized beam size is 14.7 × 6.6 milliarcseconds with a position angle of -16°. This beam is similar in size to that derived for 4C31.04 at 1.7 GHz. Parameters relevant to the maps and the source are given in Table 3. The last two columns in this table ("S_E" and "S_W") are the integrated flux densities of the eastern and western components as measured by integrating over the relevant regions in the images. The region between the lobes was excluded; see Section 3.2 for a discussion about the location of the core.

3. RESULTS

3.1 3C346

The images of 3C346 at 1.7 and 8.4 GHz are shown in Figure 3a,b,c. At 1.7 GHz we detect two components separated by ∼2.2", in agreement with Rendong *et al.* (1991), the western component being the stronger and more compact. It coincides with the core detected by Spencer *et al.* (1991). The eastern component is a bright knot in the asymmetric jet (Spencer *et al.* 1991), and is surrounded by resolved extended emission.

At 8.4 GHz, only the nuclear emission is detected at full resolution. We classify this emission as a core with a short one-sided jet, oriented towards the same side as the extended jet. The eastern knot is completely resolved in this map, but it is easily visible in the map produced at lower resolution (HPBW = 23.5 mas). The jet-counter jet brightness ratio at 8.4 GHz is $\gtrsim$20 at ∼ 2 mas from the core.

Lower resolution images of Spencer *et al.* (1991), van Breugel *et al.* (1992), and Akujor & Garrington (1993) indicate that the structure shown here is embedded in a larger halo of about 12" in extent. The compact "core" is located nearly at the center of this halo and the "knot" is a bright spot in the asymmetric jet.

The high brightness of the core is clearly illustrated in Figure 3c by its very small size at 8.4 GHz. Using the low resolution core flux density at 8.4 GHz and assuming that the peak in the 1.7 and 8.4 GHz images are coincident on the sky, then the apparent spectral index

between these two frequencies is $\alpha_{1.7}^{8.4}$ = -0.25. [1] The inverted spectrum is confirmed by data from the literature (Rendong *et al.* 1991 and Spencer *et al.* 1991). Our full resolution image at 8.4 GHz indicates that the emission in the nuclear region is dominated by the inner portion of the jet; the peak brightness at the core corresponds to only 40% of the core flux density measured from the lower resolution image. Since the core spectrum obtained from the low resolution images is inverted, then the spectrum of the inner jet must be flat or inverted.

3.2 4C31.04

The images of 4C31.04 at 1.7 and 8.4 GHz are shown in Figure 4a,b. Due to the resolution of the source on the longer baselines, the final uv coverage is similar at the two frequencies resulting in similar synthesized beam sizes. The poor uv coverage at 8.4 GHz implies that the details in the image may not be fully reliable. At 1.7 GHz the total flux density measured with the VLA was 2.51 Jy and the final VLBI CLEAN image contained 2.46 Jy, which is 98% of the total. At 8.4 GHz the total CLEAN flux density in the image was 0.79 Jy or 76% of the measured total intensity of 1.04 Jy. The missing flux density at 8.4 GHz is presumably in the larger size scales which were better sampled at 1.7 GHz. The source appears as a double; the eastern lobe is stronger and more compact than the western one which shows a distorted structure.

A faint bridge of emission is visible between the lobes at 1.7 GHz, while a faint component is present at 8.4 GHz. Although the limited uv coverage and sensitivity make the reliability of this 0.014 Jy component to be somewhat uncertain, it is supported by the presence and morphology of radio emission in this area at 1.7 GHz. In fact, this low frequency map clearly shows that the W lobe, in addition to its extension in N-S direction, has an E-W extension, i.e. in the same direction of the extension of the E lobe. At 1.7 GHz, the flux density in this region is about 0.030 Jy, which would imply a spectral index of ≈ 0.5 or flatter, since the measurement at the lower frequency probably includes some extended emission. Therefore this feature could be the location of a flat spectrum core. We note that if such a component were the core, then the ratio between the total radio power and the core radio power for this source would be in agreement with the correlation found for extended radio galaxies by Giovannini *et al.* (1988). This correlation "predicts" an unbeamed core flux density of about 17 mJy at 5 GHz, i.e. of the same order of magnitude of our core candidate. This tends to support our identification of the core and suggests that its flux density is only weakly affected by beaming effects, as is expected from the symmetric morphology of this source. However, it is not yet clear if the correlation found by Giovaninni *et al.* (1988) for radio galaxies can be used for CSO sources since the nature of these sources is still uncertain; in particular, it is not known if they are young, evolving sources.

Alternatively, the "core" of 4C31.04 could be embedded in one of the two lobes of radio emission, or even in any region in our map if its flux density were too low to be detected. The nondetection of the source on long baselines where the extended emission is completely resolved puts an upper limit of approximately 100 mJy on the flux density of the core. We find it unlikely that one of the two "lobes" is the core based on component spectra as well as size. If the brightest regions in the two images are assumed to be co-located on the sky, their spectral indices are too steep (≈ 0.6 for the E component and ≈ 0.7 for the W one). Moreover, both lobes are completely resolved by our longest baselines. We cannot exclude the presence of a faint core component imbedded in one of the two lobes (in this case the E one is favored, being stronger and with a flatter spectrum). In this case, the source

[1] $S(\nu) \propto \nu^{-\alpha}$

structure would be highly asymmetric. The spectra of the eastern and western components including data at 0.327 GHz from Wrobel & Simon (1986) are shown in Figure 5. The eastern component appears to become optically thick below about 1 GHz while the western component remains optically thin to 0.327 GHz.

No jet–like feature is visible in our maps and the two lobes are clearly extended and cannot be identified as jets or bright knots in a jet structure. Despite our incomplete uv-coverage, a jet–like structure should be easily detected at a brightness of a tenth of mJy/beam. This means that no Doppler boosted jet–like component is present in this source. We favor the hypothesis that this source shows a double structure, with two extended (at VLBI resolution), somewhat distorted lobes and a faint core emission in between.

Wrobel & Simon (1986) discuss the presence of a time variable component in this source at 15 GHz, with variations of as much as 0.4 Jy. However, we note that the radio variability is mostly due to one flux density measurement in 1979 with a large uncertainty. Marscher *et al.* (1979) classify this source as a bursting radio source at 21 cm, but 4 different VLA observations in the time range 1978 October - 1980 December show no significant flux density variability. Due also to the observed low core flux density discussed above, we think that the reported radio variability of this source is hard to believe and, if confirmed, very peculiar.

4. DISCUSSION

4.1 3C346

3C346 (B 1641+174) is identified with a 17.2 magnitude galaxy with a redshift of 0.16. The parent galaxy is in a double system with the compact, north west nucleus coincident with the radio core (Dey & van Breugel, 1994). Spectroscopic data show that it has optical properties similar to those of QSOs; it is included by Hewitt & Burbidge (1991) in their "optical catalog of extragalactic emission–line objects similar to quasi–stellar objects" and it is classified as a weak emission line radio galaxy by Fabbiano *et al.* (1984). X-ray emission was detected by the Einstein Observatory (Fabbiano *et al.* 1984). Dey & van Breugel (1994) observed excess ultraviolet light from the region of the radio knot which they interpreted as synchrotron emission from a hot spot at the end of the radio jet.

The total radio power at 408 MHz is 2.14×10^{26} W/Hz, therefore this source is in the same radio power range of extended FR-II radio galaxies (see Fanaroff & Riley 1974 for a definition of FR-I and FR-II radio galaxies). The large scale radio structure has been discussed by Spencer *et al.* (1991), Akujor *el al.* (1991), van Breugel *et al.* (1992), and Akujor & Garrington (1993). It consists of a compact, core component from which a jet emerges toward the east, extending with some wiggles and bright knots for ∼4.5". An extended cocoon is present both around the jet and on the opposite side, for a total extent of ∼12". This structure suggested to Spencer *et al.* (1991) that this source is a large source viewed nearly end on. Rendong *et al.* (1991) made VLBI observations at 0.6 GHz and fitted a two component model with a separation of 2.2 arcsecond in a position angle of 80°.

The presence of relativistic jets in strong radio sources as quasars and FR-II radio galaxies is now widely accepted (see Antonucci, 1993 for a recent review). This hypothesis is now also supported by recent results on FR-I radio galaxies (Parma *et al.* 1994; Capetti *et al.* 1995) which show that the jet asymmetry is large close to the core and reduces gradually at larger distance as expected for intrinsically symmetric jets in which velocity decreases with the distance from the core. Since a milliarcsecond one-sided jet is visible in our map in the same direction of the large scale one-sided jet found by Spencer *et al.* (1991), we interpret the one-sided jet as due to a symmetric structure affected by Doppler favoritism. We will use the available data to constrain the possible values of the intrinsic jet velocity and of the

orientation of the radio source with respect to the line of sight.

Following Giovannini *et al.* (1994), we can constrain the jet velocity β and orientation to the line of sight θ in three different ways. The first method assumes that the milliarcsecond jets are intrinsically symmetric, and boosted by Doppler favoritism. From the jet to counter–jet brightness ratio R ($\gtrsim$20) we obtain in this case a lower limit to $\beta cos\theta$ of 0.54 (see Giovannini *et al.* 1994 and references therein for a more detailed discussion on this method). The allowed region in the $\theta - \beta$ space is shown in Figure 6.

The second independent constraint may be derived using the prominence of core radio power with respect to the total radio power. We will use the correlation found by Giovannini *et al.* (1988). This correlation has been derived with no selection by source size and can be used for sources with quasar–like strong cores. It allows the derivation of the beaming enhancement necessary to account for the core prominence in the unified scheme models. The measured core power of 3C346 is 22.4 times larger than that expected from the core versus total radio power relation, leading to the allowed region for $\theta - \beta$ again drawn in Figure 6 (see Giovannini *et al.* 1994 for a more detailed discussion on this method).

The third method compares the X-ray detected emission with that expected by the Self Compton Model (Ghisellini *et al.* 1993, Marscher 1987). With available data, this method is inconclusive, since it leads to a lower limit to the Doppler factor $\delta \gtrsim 0.1$. This does not allow any constraint on the jet velocity or orientation angle with respect to the line of sight.

From Figure 6 the allowed region for β and θ is $\theta < 32^\circ$ and $\beta > 0.8$, so we conclude that this source is at a small angle to the line of sight. Unified scheme models predict that sources with a steep spectrum (i.e. 'lobe dominated') and with an angle with respect to the line of sight $10^\circ < \theta < 40^\circ$ should be classified as steep spectrum QSS or broad line radio galaxies (see e.g. Ghisellini *et al.* 1993). This is in agreement with the optical properties similar to those of QSOs reported in literature for 3C346 (see Sect. 4.1), but it is in contrast with the lack of broad emission lines in its spectrum. However, Dey & van Breugel (1994), infer a large optical extinction ($A_v > 8$) for this galaxy which could explain the lack of detection of the broad line region, and suggest that this region might only be visible in the infrared.

The projected angular size of this source is $\sim$ 12" corresponding to a linear size of 21.4 kpc. An angle of $\theta < 30^\circ$ with respect to the line of sight implies an intrinsic linear size of $>$ 43 kpc. In a size-power diagram (see e.g. De Ruiter *et al.* 1990) a source with the radio power of 3C346 is expected to have a linear size between 50 and 500 kpc. Therefore, the deprojected lower limit on the size obtained for 3C346 ($>$ 43 kpc) is on the low end of the range but not peculiar. This strongly suggests that 3C346 does not belong in the CSS class, but is a common FR–II radio galaxy foreshortened by projection. In this scenario, the "knot" visible at low resolution in our images would correspond to the "hot spot" at the end of the jet. Detection of superluminal motion in the core would further strengthen this conclusion.

4.2 4C31.04

4C31.04 (B 0116+319) is identified with the bright elliptical galaxy MCG 5-4-18 (Caswell & Wills 1967), a member of a close pair of galaxies, with a redshift of z=0.059 (Heckman *et al.* 1983). Van den Bergh (1970) reports [OII] emission in 4C31.04 and Heckman *et al.* (1983) describe this source as showing low excitation forbidden oxygen lines as well as a non stellar continuum optical and infrared source. Mirabel (1990) reports the detection of HI absorption in this galaxy and a high-velocity cloud of atomic hydrogen against the nuclear compact continuum radio source at the galaxy center. Marscher *et al.*

(1979) failed to detect X-ray using HEAO 2.

The total radio power at 408 MHz is 1.26×10^{25} W/Hz i.e. in the same range of the most powerful FR-I radio galaxies. Perley (1982) indicates that the radio source is smaller than 1" in extent. Wrobel & Simon (1986) presented a 0.327 GHz VLBI map where the source is a double separated by about 0.07". Kulkarni & Romney (1990) give results from a three antenna VLBI array at 1.4 GHz also giving a double with a separation of 0.07".

The parsec scale structure of this source consists of two almost equal flux density components, which are resolved by the longest baselines. These show some distortion, but the overall structure is rather symmetric. This source is clearly different from most of the VLBI sources found in the literature and in our sample (see Giovannini *et al.* 1994, and references therein), in which a core-jet structure is dominant. Both components have a clearly extended radio structure which do not satisfy the generaly accepted jet definition (Bridle & Perley, 1984). They resemble two extended lobes very similar to those found in radio galaxies at a much larger scale. The interpretation of the morphology of 4C31.04 is not straightforward. Sanghera & Spencer (1993) suggest that strong interactions with the ISM may explain the small size and distorted appearance of many CSS sources associated with quasars.

The line emission reported by Vanden Bergh (1970) and Heckman *et al.* (1983) are relatively weak compared to other radio galaxies with compact radio sources. Therefore, there is no compelling evidence of a strong interaction of the radio jets with the ambient medium. The apparent small size could then be due simply to the source being young, but this alone does not explain its rather distorted appearance. Another possibility is to invoke some other effects such as precession, although the source does not show the symmetry expected from such a model, or from some simple motion of the core.

Another possible cause of the apparent distortion of the structure of 4C31.04 could be gas flow inside the galaxy as is reported in NGC4874 by Feretti & Giovannini (1985) on a larger scale. Gas infalling from tidal interactions with the other galaxy of this double system could provide systematic gas flow in the nuclear region. Mirabel (1990) reports observations of HI inflow in absorption against the continuum source which indicate a considerable amount of HI gas in the central region of this giant elliptical galaxy. Normal elliptical galaxies are rather poor in interstellar gas so infalling gas could result in systematic gas motions even at the nucleus.

The symmetric radio structure of this source is reminiscent of that of the CSOs (see Readhead *et al.* 1994 for a recent review), which are very luminous, small, and short-lived objects. Prototypes of this class are 0108+388 (Conway *et al.* 1994), 0710+439 and 2352+495 (Conway *et al.* 1992, Wilkinson *et al.* 1994). In table 4 we compare the physical parameters of 4C31.04 and 2352+495. 4C31.04 is at a much lower redshift and has a lower radio power, linear size and equipartition magnetic field strength than 2352+495. The equipartition minimum pressure within the radio emitting regions, 0.63 U_{min} (see Feretti *et al.* 1992), is lower than that of canonical CSOs, therefore the two lobes could be statically confined by the external pressure present in the Narrow Line region.

In a discussion of CSOs, Wilkinson *et al.* (1994) point out that the well studied CSOs 2352+495 and 0710+439 have very strong similarities: both are identified with galaxies with narrow emission lines and not broad emission lines. Host galaxies have distorted isophotes and nearby companions. The radio emission has a low percentage of polarized flux density. The host galaxy of 4C31.04 is a member of a double galaxy system and its optical properties are similar to the CSOs host galaxies. Moreover, the 8.4 GHz polarization measured using the VLA during calibration observations give a low polarization of $0.56 \pm 0.02\%$. These

properties of 4C31.04 strengthen the argument for its interpretation as a symmetric source. We conclude that 4C31.04 could represent a nearby and faint member of the CSO class.

5. CONCLUSIONS

The prominence of the high brightness, compact core seen in 3C346 together with the large scale structure of the radio emission and absence of a counter jet are evidence that this source is viewed nearly end on and may not be confined to its host galaxy. The optical properties of the host galaxy are in agreement with the expectations of unified scheme models.

4C31.04 is a more difficult case to analyze. There is not a prominent flat spectrum high brightness "core" at the epoch of these observations and no jet–like feature is evident in our maps. This would argue against Doppler boosting due to a relativistic jet being significant and thus against the source being seen end on. Although with the current data it is not possible to firmly establish the core location, we favor the hypothesis that the core is located between the main components and that this source has relatively symmetric structure. The morphology and physical properties suggest that this source could be a low redshift Compact Symmetric Object. The existence of a nearby member of this class of objects is very interesting and, even if more data are necessary to confirm the absence of relativistic motions and to confirm the core identification in 4C31.04, its physical properties suggest that CSO sources might be present also at our epoch and not only in high power and high redshift sources. Therefore, it has to be taken into account in future statistical tests studing the cosmological evolution of CSOs and the possible connection between CSOs and extended radio galaxies.

If 4C31.04 is not affected by projection, then the distortions of the structure must be intrinsic. These could be due to ram pressure of a high velocity gas flowing into the nuclear region of the parent galaxy as observed by Mirabel (1990).

Acknowledgements

We would like to thank A.C.S. Readhead for useful discussions and the staffs of the observatories who participated in these observations and especially to the staff of the Cal Tech VLBI correlator. The National Radio Astronomy Observatory is operated by Associated Universities, Inc. under a cooperative agreement with the National Science Foundation.

References

Akujor, C. E., & Garrington, S. T. 1993 in Sub-arcsecond Radio Astronomy, ed. R. J. Davis & R. S. Booth (Cambridge: Cambridge University Press), p. 275

Akujor, C. E., Spencer, R. E., Zhang, F. J., Davis, R. J., Browne, I. W. A., and Fanti, C. 1991, *M.N.R.A.S* **250**, 214

Antonucci, R. R. J. 1993, *Ann. Rev. Astr. Ap.* **31**, 473

Capetti, A., Fanti, R., Parma, P. 1995 *Astr. Ap.* in press

Caswell, J. L., & Wills, D. 1967, *M.N.R.A.S.* **135**, 231

Conway, J.E., Myers, S.T., Pearson, T.J., Readhead, A.C.S., Unwin S.C., and Xu, W. 1994, *Ap. J*, in press

Conway, J.E., Pearson, T.J., Readhead, A.C.S., Unwin, S.C., Xu, W., and Mutel, R.L. 1992, *Ap. J.* **396**, 62

De Ruiter, H.R., Parma, P., Fanti, C., and Fanti, R. 1990, *Astr. Ap.* **227**, 351

Dey, A., & van Breugel, W. J. M., 1994, *Astron. J.*, **107**, 1977

Fabbiano, G., Miller, L., Trinchieri, G., Longair, M., and Elvis, M. 1984, *Ap. J.*, **277**, 115

Fanaroff, B. L., & Riley, J. M. 1974 *M.N.R.A.S.* **167**, 31

Fanti, R., Fanti, C., Schilizzi, R. T., Spencer, R. T., Rendong, N., Parma, P., van Breugel, W. J. M., and Venturi, T. 1990, *Astr. Ap.* **231**, 333

Feretti, L., & Giovannini, G. 1985, *Astr. Ap.* **147**, L13

Feretti, L., Perola, G. C., and Fanti, R. 1992, *Astr. Ap.* **265**, 9

Giovannini, G., Feretti, L., Gregorini, L., and Parma, P. 1988, *Astr. Ap.* **199**, 73

Giovannini, G., Feretti, L., and Comoretto, G. 1990, *Ap.J.*, **358**, 159

Giovannini, G., Feretti L., Venturi, T., Lara, L., Marcaide, J., Rioja, M., Spangler, S.R., and Wehrle, A.E., 1994, *Ap. J.*, in press

Ghisellini, G., Padovani, P., Celotti, A., and Maraschi, L., 1993, *Ap. J.* **407**, 65

Heckman, T. M., Lebofsky, M. J., Rieke, G. H., and van Breugel, W., 1983, *Ap. J.*, **272**, 400

Hewitt, A., & Burbidge, G., 1991, *Ap.J.Suppl.*, **75**, 297

Kulkarni, V. K., & Romney, J. D. 1990 in Compact Steep-Spectrum and GHz-Peaked Spectrum Radio Sources, eds. C. Fanti, R. Fanti, C. P. O'Dea and R. T. Schilizzi, CNR, Bologna, 85

Marscher, A. P., Marshall, F. E., Mushotzky, R. F., Dent, W. A., Balonek, T. J., and Hartman, M. F. 1979, *Ap. J.*, **233**, 498

Marscher, A.P., 1987, in *Superluminal Radio Sources*, J.A. Zensus & T.J. Pearson Eds., Cambridge University Press, p. 280

Mirabel, I.F., 1990, *Ap.J.(Letters)*, **352**, L37

Parma, P., de Ruiter, H. R., Fanti, R., Laing, R. 1994 in *The First Stromlo Symposium: The Physics of Active Galaxies*, G.V. Bicknell, M.A. Dopita, P.J. Quinn Eds., p. 241

Peacock, J. A., & Wall, J. V. 1982, *M.N.R.A.S.* **198**, 843

Pearson, T.J., 1991, *BAAS*, **23**, 991

Perley, R. A. 1982, *A. J.*, **87**, 859

Readhead, A.C.S., Xu, W., Pearson, T.J., Wilkinson, P.N., and Polatidis, A.G. 1994, in Compact Extragalactic Radio Sources, Ed. J.A. Zensus & K.I. Kellerman, p. 17

Readhead, A.C.S., Xu, W., Pearson, T.J., Wilkinson, P.N., and Polatidis, A.G. 1995, in preparation

Rendong, N., Schilizzi, R. T., Fanti, C., and Fanti, R. 1991, *Astr. Ap.* **252**, 513

Sanghera, H. S. & Spencer, R. E. 1993 in Sub-arcsecond Radio Astronomy, ed. R. J. Davis & R. S. Booth (Cambridge: Cambridge University Press), 367

Schwab, F. R., & Cotton, W. D. 1983 *A.J.*, **88**, 688

Spencer, R. E., Schilizzi, R. T., Fanti, C., Fanti, R., Parma, P., van Breugel, W. J. M., Venturi, T., Muxlow, T. W. B., and Rendong, N. 1991, *M.N.R.A.S* **250**, 225

Van Breugel, W. J. M., Fanti, C., Fanti, R., Stanghellini, C., Schilizzi, R. T., and Spencer, R. E. 1992, *Astr. Ap.* **256**, 56

Van den Bergh, S. 1970 *Pub. A. S. P.* **82**, 1374

Wilkinson, P. N., Polatidis, A. G., Readhead, A. C. S., Xu, W., and Pearson, T. J. 1994, *Ap. J.(Letters)*, **432**, L87

Wrobel, J. M., & Simon, R. S. 1986, *Ap.J.*, **309**, 593

Figure 1: a) The uv coverage for 3C346 at 1.7 GHz.
b) The uv coverage for 3C346 at 8.4 GHz. In both figures only the final data used to obtain the published maps are drawn, points deleted as bad by editing or in the self calibration cycles are not shown.

Figure 2: a) The uv coverage for 4C31.04 at 1.7 GHz.
b) The uv coverage for 4C31.04 at 8.4 GHz. In both figures only the final data used to obtain the published maps are drawn, points deleted as bad by editing or in the self calibration cycles are not shown.

Figure 3: a) 3C346 at 1.7 GHz. The peak flux density is 149 mJy and the contours are at -1, 1, 2.5, 5, 10, 25, 50, and 95 percent of the peak. The RMS in a empty region of the image is 0.25 mJy. The restoring beam is 45 × 45 milliarcseconds.
b) Low resolution image of "knot" in 3C346 at 8.4 GHz; tick marks are every 50 milliarcseconds. The peak flux density is 6.2 mJy/beam and the contours are at -1, 1, 2, 3, 4, 5, and 6 mJy. The RMS noise is 0.25 mJy and the restoring beam is 23.5 × 23.5 milliarcseconds.
c) Full resolution image of "core" of 3C346 at 8.4 GHz; tick marks are every milliarcsecond. The peak flux density is 86 mJy and the contours are at -2.5, 2.5, 5, 10, 25, 50, and 95 percent of the peak. The RMS noise is 1.2 mJy and the restoring beam is 2.5 × 1 milliarcsecond at a position angle of 0^o.

Figure 4: a) 4C31.04 at 1.7 GHz. The peak flux density is 472 mJy and the contours are at -1, 1, 3, 5, 7, 10, 20, 30, 50, 70, 90 percent of the peak. The RMS in a empty region of the image is 1.5 mJy. The restoring beam is 17 × 10 milliarcseconds at a position angle of 72^o. The cross marks the approximate location of the possible "core" seen in b).
b) 4C31.04 at 8.4 GHz on the same scale as a). The peak flux density is 201 mJy and the contours are at -3, 3, 5, 7, 10, 20, 30, 50, 70, 90 percent of the peak. The RMS noise is 1.9 mJy. The restoring beam is 15 × 7 milliarcseconds at a position angle of -16^o.

Figure 5: The integrated spectra of the eastern and western components of 4C31.04. The 0.327 GHz measurements are from Wrobel and Simon (1986); the other values are derived from integrals over the relevant components in the images presented here. The region between the two major components is not included. The lines are shown to distinguish the two components and are not fitted spectra.

Figure 6: This figure shows the jet velocity, beta (β), versus orientation to the line of sight, theta (θ), plot for 3C346. Curved lines marked "A" are derived from the observed core dominance and the line marked "B" from the jet / counter-jet ratio. The disallowed regions are marked with diagonal stripes.

Table 1: Observations

Source	Frequency GHz	Stations	Obs. Date	Obs. Time (hours)
3C346	1.7	Y1,PT,KP,LA,FD,NL,BR,OV	1992 Jan 31	6.5
3C346	8.4	Y1,PT,KP,LA,FD,NL,BR,OV,L,N	1992 Jan 24	6.5
4C31.04	1.7	Y1,PT,KP,LA,FD,NL,BR,OV,L	1992 Jan 30, Feb 2	9.0
4C31.04	8.4	Y1,PT,KP,LA,FD,NL,BR,OV,M,N	1992 Jan 23-25	9.0

Notes: L: 32m, Medicina (Italy); M: 34m, DSS65, Robledo (Spain); N: 32m, Noto (Italy); Y1: 25m one telescope VLA (USA); PT: 25m, VLBA-Pie Town (USA); KP: 25m, VLBA-Kitt Peak (USA); LA: 25m, VLBA-Los Alamos (USA); FD: 25m, VLBA-Fort Davis; NL: 25m, VLBA-North Liberty; BR: 25m, VLBA-Brewster; OV: 25m, VLBA-Owens Valley

Table 2: Map and Source parameters for 3C346

Source	Freq. GHz	HPBW mas	(PA) deg	noise mJy/beam	S_T mJy	S_c mJy	S_{jet} mJy	PA_{jet} o
3C346	1.7	45x45	-	0.25	361	149	215	81
3C346	8.4	23.5x23.5	-	0.25	252	223	42	81
3C346	8.4	2.5x1	0	1.2	143	86		

Table 3: Map and Source parameters for 4C31.04

Source	Freq.	HPBW	(PA)	noise	S_T	S_c	S_E	S_W
	GHz	mas	deg	mJy/beam	mJy	mJy	mJy	mJy
4C31.04	1.7	17x10	72	1.5	2460	(< 30)	1366	961
4C31.04	8.4	15x7	-16	1.9	790	(14)	541	264

Table 4: Physical Parameters of Selected CSOs

Name		z	P_T^{408}	Size	U_{min}	H_{eq}
			W/Hz	pc	10^{-6} erg/cm^3	10^{-3} gauss
4C31.04		0.057	1.3×10^{25}	70		
	East				0.4	2.1
	West				0.3	1.9
2352+495		0.237	1.6×10^{26}	150		
	North Lobe				3	6
	South Lobe				2	5

Note: 2352+495 data are from Readhead *et al.* 1995.

FIGURE 1a

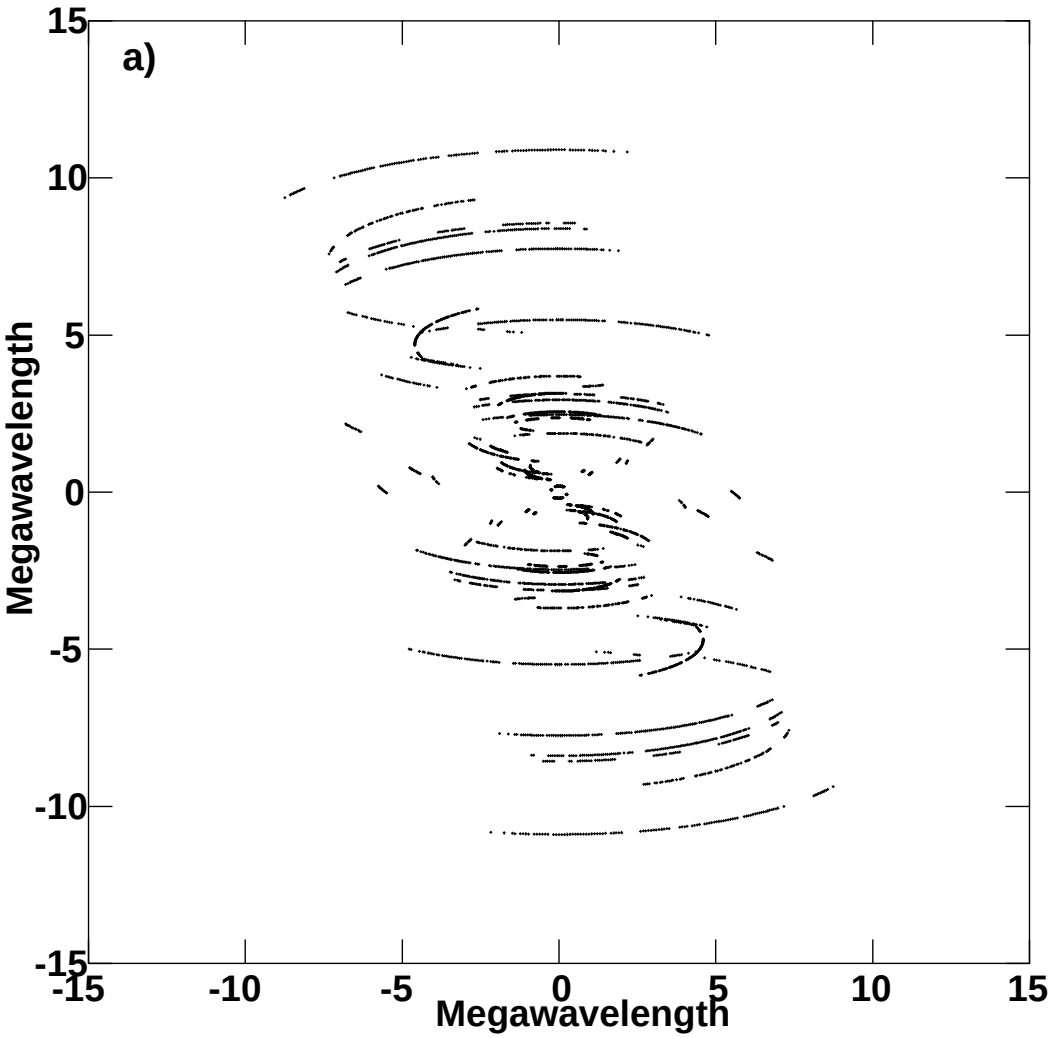
a)
15
10
5
0
-5
-10
-15
Megawavelength
-15
-10
-5
0
5
10
15
Megawavelength

FIGURE 1b

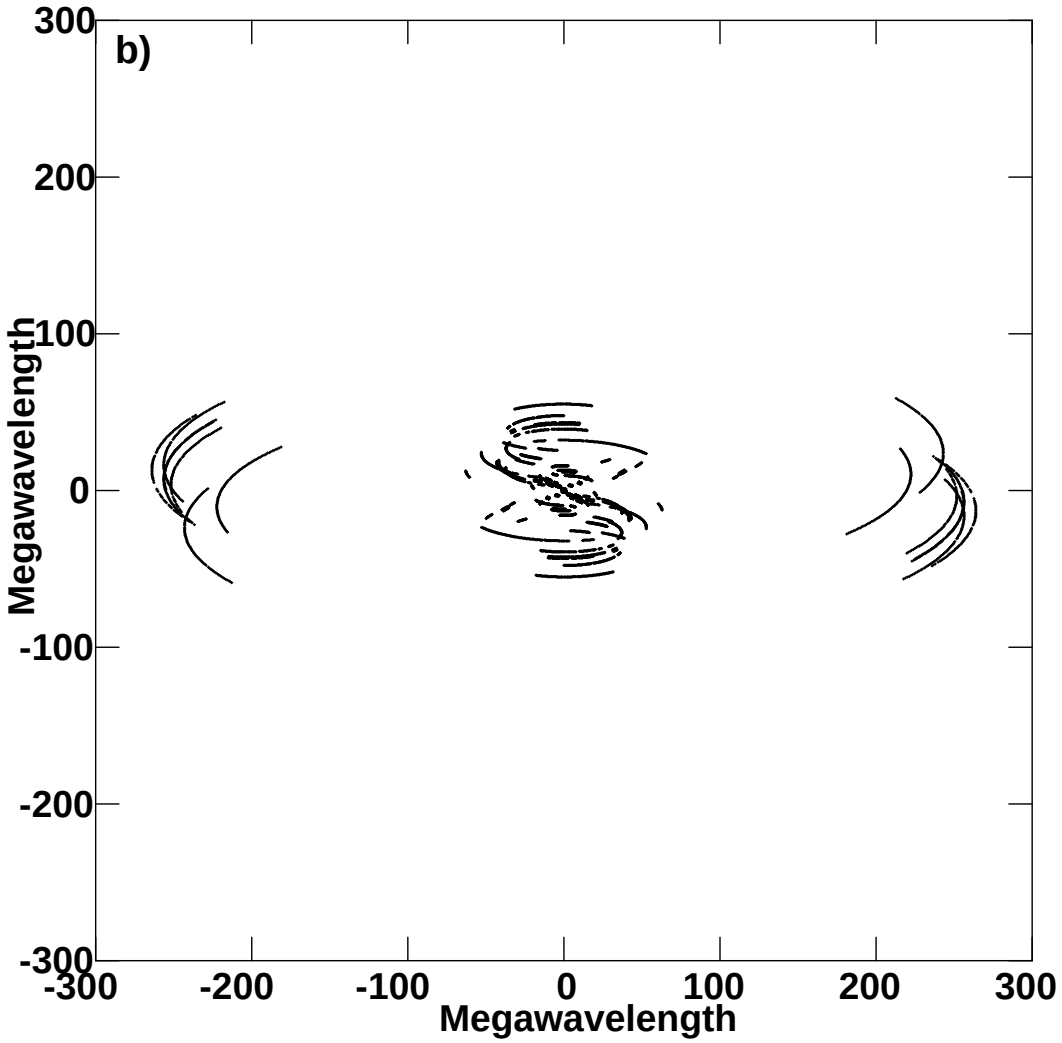
b)
300
200
100
0
-100
-200
-300
Megawavelength
-300
-200
-100
0
100
200
300
Megawavelength

FIGURE 2a

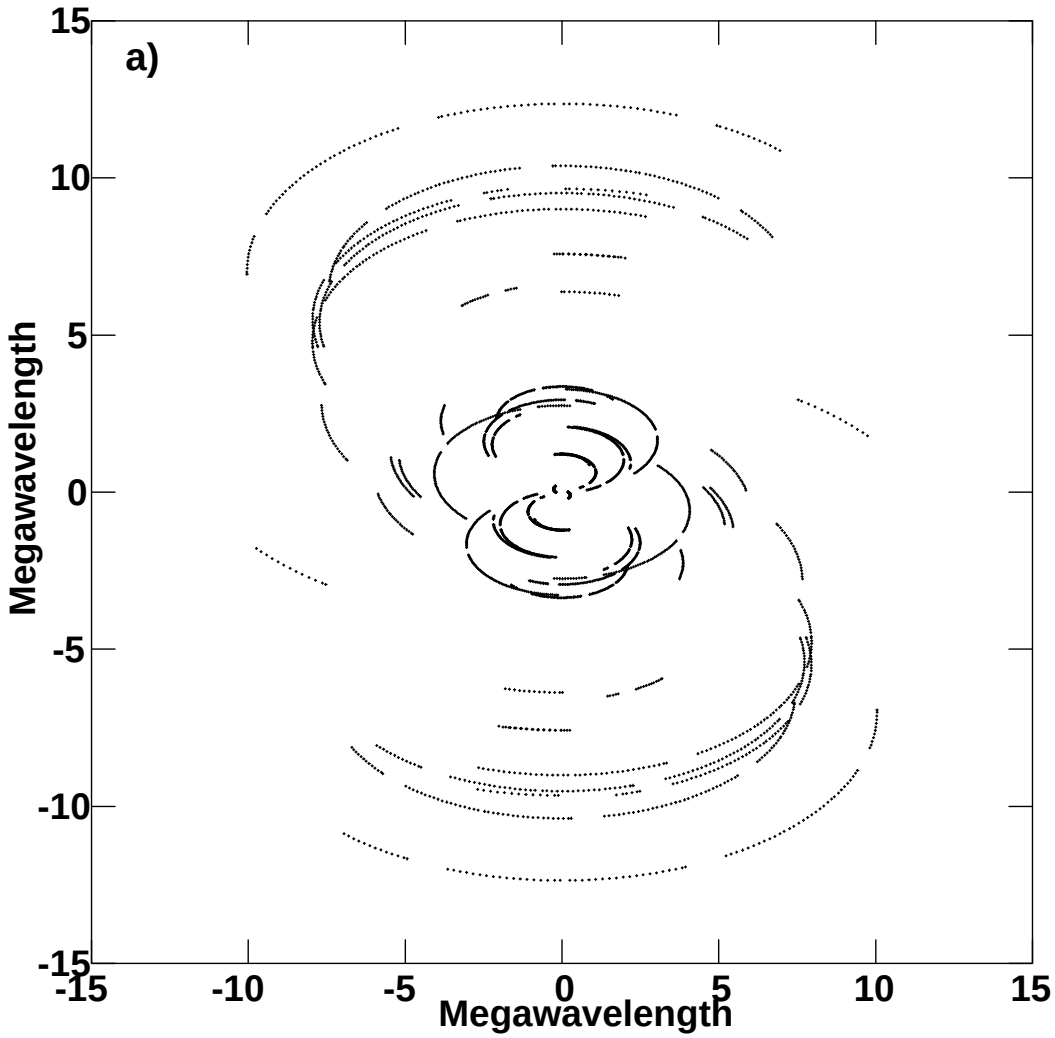
a)
15
10
5
0
-5
-10
-15
Megawavelength
-15
-10
-5
0
5
10
15
Megawavelength

FIGURE 2b

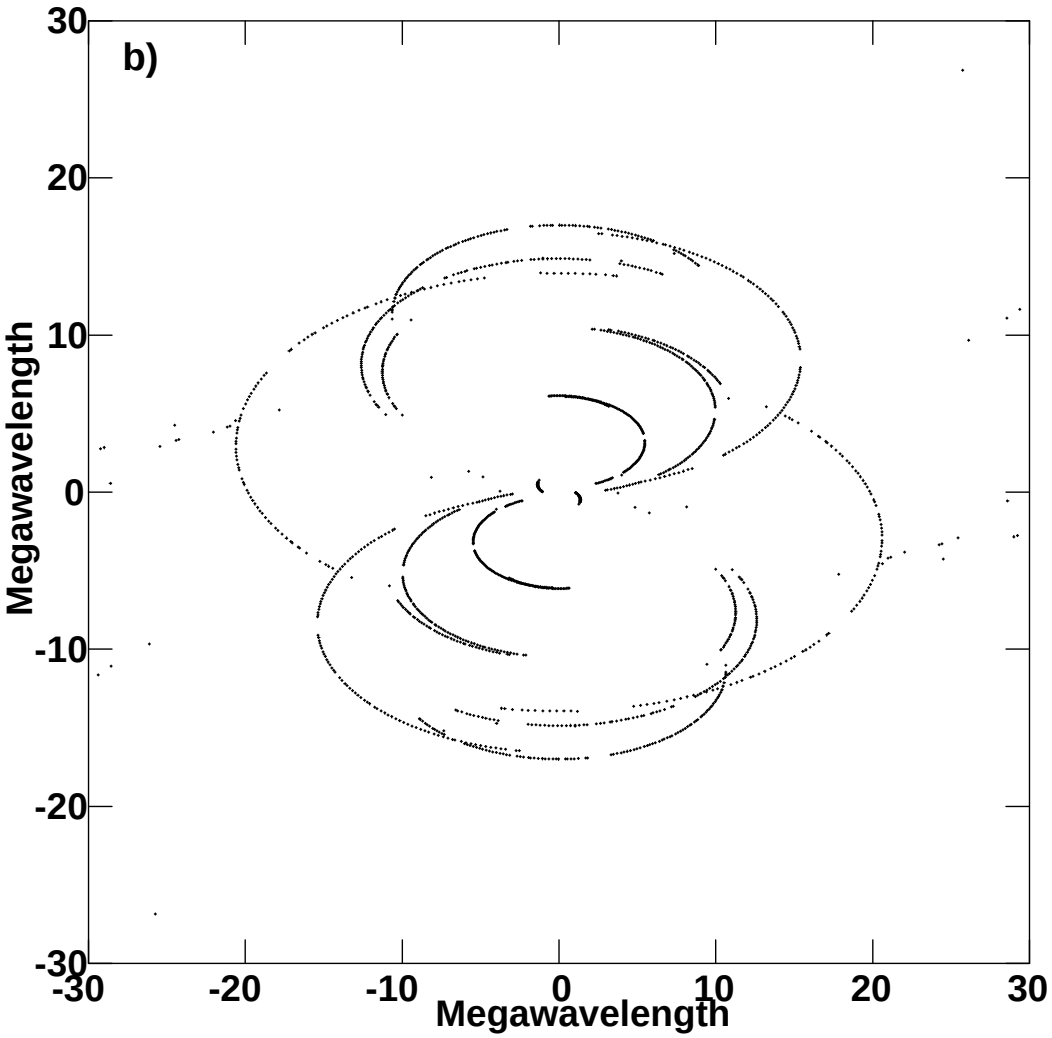
b)
30
20
10
0
-10
-20
-30
Megawavelength
-30
-20
-10
0
10
20
30
Megawavelength

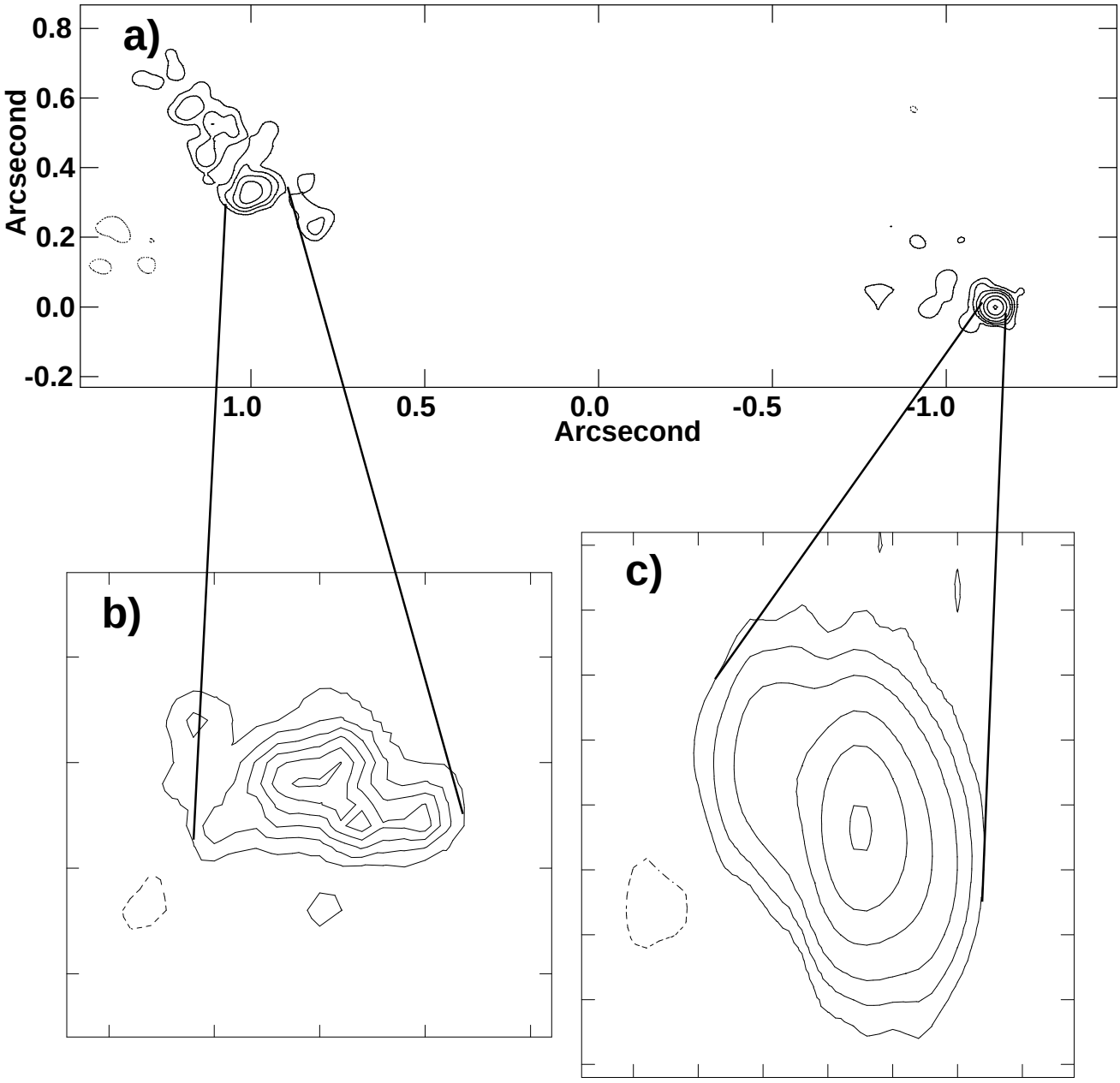

FIGURE 3

FIGURE 4a

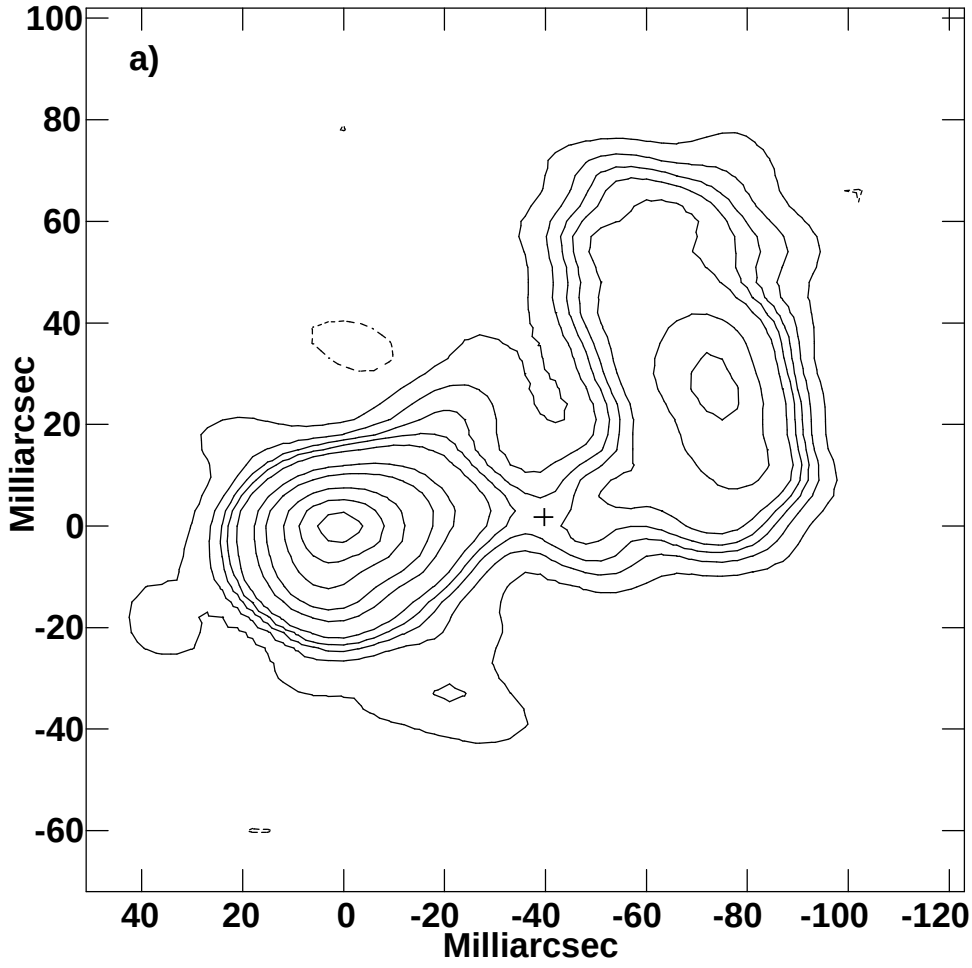
a)
100
80
60
40
20
0
-20
-40
-60
Milliarcsec
40
20
0
-20
-40
-60
-80
-100
-120
Milliarcsec

FIGURE 4b

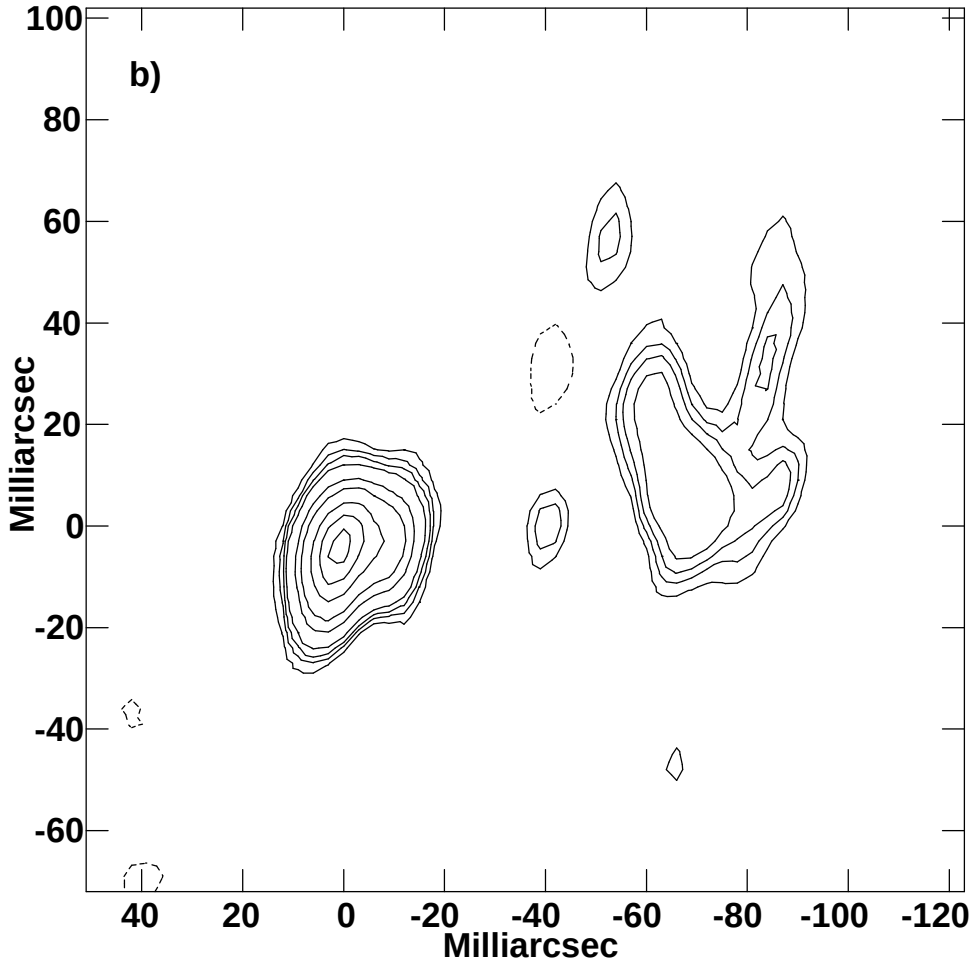
b)
100
80
60
40
20
0
-20
-40
-60
Milliarcsec
40
20
0
-20
-40
-60
-80
-100
-120
Milliarcsec

FIGURE 5

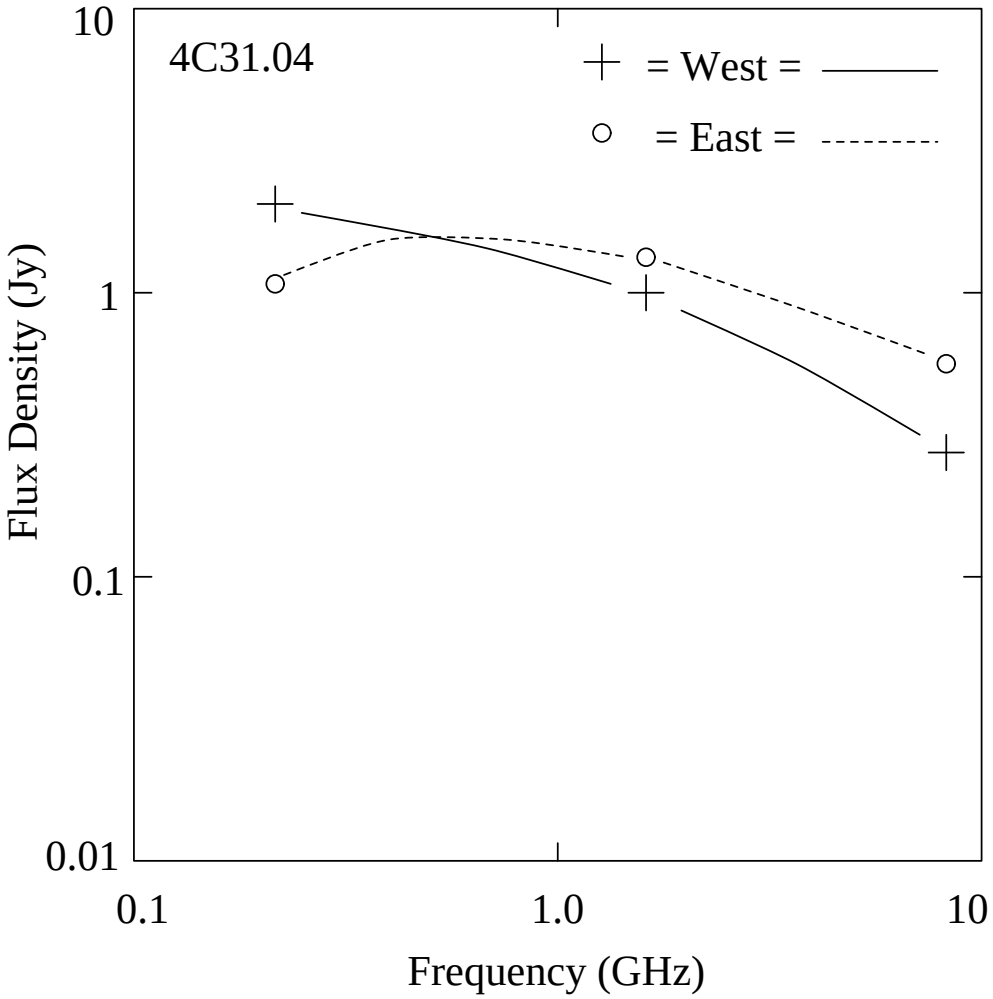
4C31.04
= West =
= East =
Flux Density (Jy)
10
1
0.1
0.01
0.1
1.0
10
Frequency (GHz)

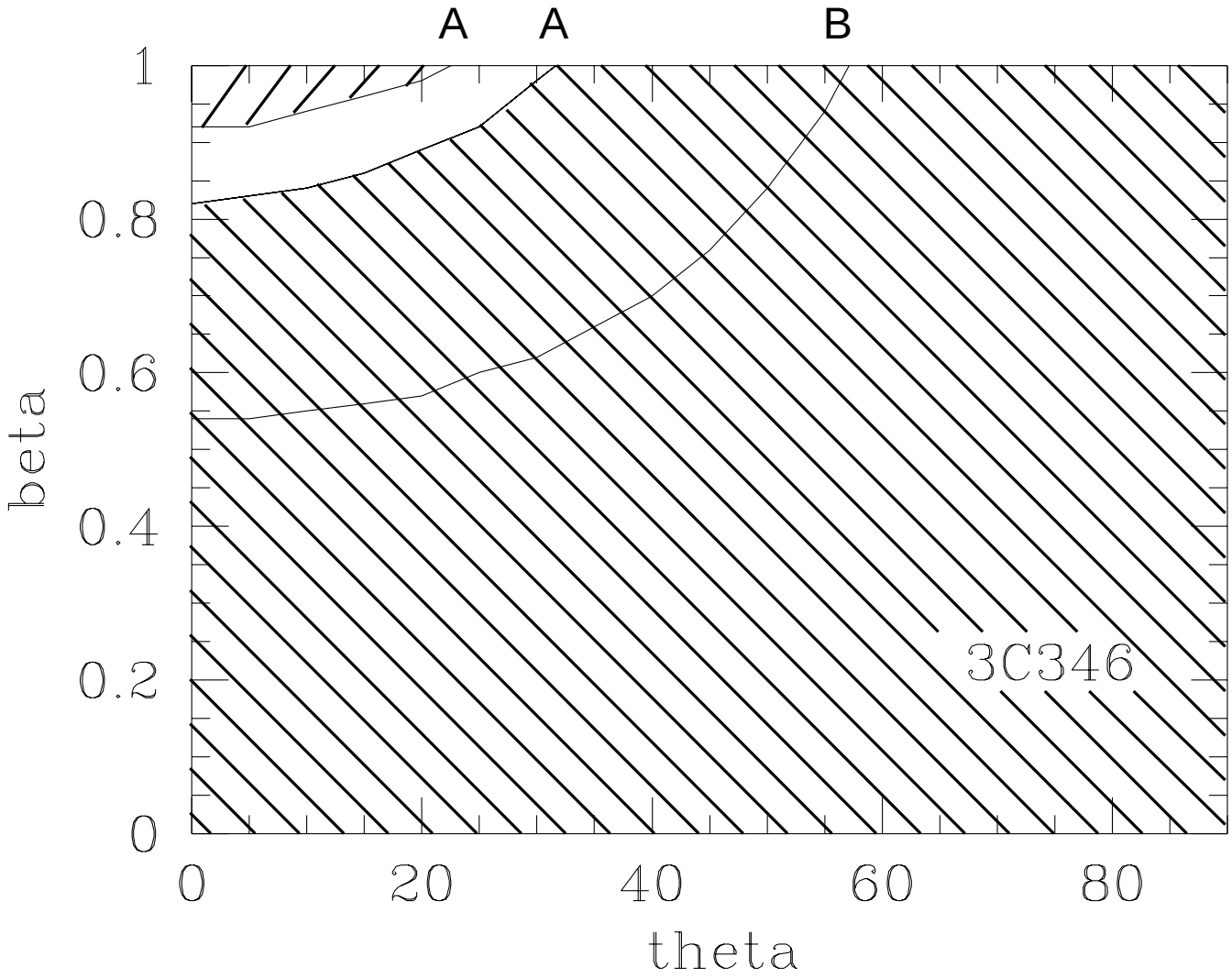
A
A
B
1
0.8
0.6
0.4
0.2
0
beta
0
20
40
60
80
theta
3C346